View metadata, citation and similar papers at core.ac.uk

brought to you by CORE

provided by UNT Digital Library

SANDIA REPORT
SAND2007-2391
Unlimited Release
Printed May 2007

Hydrocarbon Characterization Experiments in Fully Turbulent Fires

Allen J. Ricks and Thomas K. Blanchat

Prepared by
Sandia National Laboratories
Albuquerque, New Mexico 87185 and Livermore, California 94550

Sandia is a multiprogram laboratory operated by Sandia Corporation,
a Lockheed Martin Company, for the United States Department of Energy's
National Nuclear Security Administration under Contract DE-AC04-94AL85000.

Approved for public release; further dissemination unlimited.

Issued by Sandia National Laboratories, operated for the United States Department of Energy by Sandia Corporation.

NOTICE: This report was prepared as an account of work sponsored by an agency of the United States Government. Neither the United States Government, nor any agency thereof, nor any of their employees, nor any of their contractors, subcontractors, or their employees, make any warranty, express or implied, or assume any legal liability or responsibility for the accuracy, completeness, or usefulness of any information, apparatus, product, or process disclosed, or represent that its use would not infringe privately owned rights. Reference herein to any specific commercial product, process, or service by trade name, trademark, manufacturer, or otherwise, does not necessarily constitute or imply its endorsement, recommendation, or favoring by the United States Government, any agency thereof, or any of their contractors or subcontractors. The views and opinions expressed herein do not necessarily state or reflect those of the United States Government, any agency thereof, or any of their contractors.

Printed in the United States of America. This report has been reproduced directly from the best available copy.

Available to DOE and DOE contractors from
U.S. Department of Energy
Office of Scientific and Technical Information
P.O. Box 62
Oak Ridge, TN 37831

Telephone: (865) 576-8401
Facsimile: (865) 576-5728
E-Mail: reports@adonis.osti.gov
Online ordering: http://www.osti.gov/bridge

Available to the public from
U.S. Department of Commerce
National Technical Information Service
5285 Port Royal Rd.
Springfield, VA 22161

Telephone: (800) 553-6847
Facsimile: (703) 605-6900
E-Mail: orders@ntis.fedworld.gov
Online order: http://www.ntis.gov/help/ordermethods.asp?loc=7-4-0#online

SAND2007-2391
Unlimited Release
Printed May 2007

Hydrocarbon Characterization Experiments in Fully Turbulent Fires

Allen J. Ricks and Thomas K. Blanchat
Fire Science and Technology Department
Sandia National Laboratories
PO Box 5800
Albuquerque, NM 87185

Abstract

As the capabilities of numerical simulations increase, decision makers are increasingly relying upon simulations rather than experiments to assess risks across a wide variety of accident scenarios including fires. There are still, however, many aspects of fires that are either not well understood or are difficult to treat from first principles due to the computational expense. For a simulation to be truly predictive and to provide decision makers with information which can be reliably used for risk assessment the remaining physical processes must be studied and suitable models developed for the effects of the physics. The model for the fuel evaporation rate in a liquid fuel pool fire is significant because in well-ventilated fires the evaporation rate largely controls the total heat release rate from the fire. A set of experiments are outlined in this report which will provide data for the development and validation of models for the fuel regression rates in liquid hydrocarbon fuel fires. The experiments will be performed on fires in the fully turbulent scale range (> 1 m diameter) and with a number of hydrocarbon fuels ranging from lightly sooting to heavily sooting. The importance of spectral absorption in the liquid fuels and the vapor dome above the pool will be investigated and the total heat flux to the pool surface will be measured. The importance of convection within the liquid fuel will be assessed by restricting large scale liquid motion in some tests. These data sets will provide a sound, experimentally proven basis for assessing how much of the liquid fuel needs to be modeled to enable a predictive simulation of a fuel fire given the couplings between evaporation of fuel from the pool and the heat release from the fire which drives the evaporation.

CONTENTS

FIGURES

TABLES

NOMENCLATURE

CARS	coherent anti-Stokes Raman scattering
CGA	Combustion Gas Analyzer
DAS	data acquisition system
FRH	FLAME/Radiant Heat
HP	Hewlett-Packard
MUX	more multiplexer unit
NI	National Instruments
SNL	Sandia National Laboratories
TTC	Thermal Test Complex

1. INTRODUCTION

Fuel evaporation rates from large liquid pool fires have been studied for several decades (see Hottel [1959], Babrauskas [1983], Koseki [1989], Koseki and Mulholland [1991], Koseki and Iwata [2000], Chatris et al. [2001], and Muñoz et al. [2004]). Fuel regression rates show a dependence upon fire diameter, fuel type, and ambient conditions including temperature and wind speed. Babrauskas [1983] presented a review of experimental data for large hydrocarbon fires and discussed the effects of pan diameter, pan lip height, and wind speed. Typical scatter in experimental data reported in the review of Babrauskas [1983] for mean, steady-state fuel regression rates for a given fuel under quiescent conditions appears to be approximately ±10% of the measurement.

Among the studies of fuel regression in smaller-scale fires the work of Hamins et al. [1994] is notable because the fuel regression rates were correlated with heat fluxes to the pool. Hamins measured the liquid reflectivity, heat fluxes, and burning rates in concentric rings within a 30 cm fire fueled by methanol, heptane, toluene, or methyl methacrylate. Both the total and the radiative heat fluxes to the pool were studied as a function of both angle and radial location in the pool. The radiation data were not spectrally resolved, and the importance of convection within the pool was not studied.

Fuel regression rate models have recently been incorporated in numerical simulations (see Novozhilov and Koseki [2004], and Prasad et al. [1999]). These modeling efforts have primarily been directed towards relatively small fires (< 1 m diameter) which are not in the fully turbulent regime. Since fire size and intensity are largely controlled by the fuel evaporation rate, improvement in the modeling of fuel evaporation rates in large, fully turbulent fires is a topic of considerable practical interest.

An assessment of the current state of knowledge about physical processes important to predictions of fuel regression rates in pool fires has recently been conducted by Brown et al. [2006]. Several of the physical processes discussed by Brown et al. will be studied in the present work, including convection within the pool and absorptivity in the liquid fuel and fuel vapor. Of these phenomena, the absorptivity in the fuel vapor in a fire stands out because it is believed that the fuel regression rates are strongly dependent upon the radiant heat flux incident on the surface of the pool, and that heat flux is controlled not only by the emission within the fire but also the absorption above the surface of the pool.

1.1 Experiment Objective

The objectives of the present experiments are:

1. Measure the spectral reflectivity at the fuel-air interface and the spectral transmissivity in liquid fuels over depths of order millimeters for a range of liquid fuels, including easily simulated, well characterized mixtures of simple fuels as well as fuels in practical use such as JP-8
2. Measure the fuel regression rates for a variety of liquid hydrocarbon fuels in a quiescent environment

3. Measure the spectral absorption coefficients of the fuel/product mixture in the vapor dome above the pool surface
4. Measure the total heat flux (convection and incident radiation) integrated across the surface of the pool to investigate the connection between the integral heat flux and the fuel regression rate
5. Determine the importance of large scale convective transport within the liquid fuel to the fuel regression rate

A brief overview describing how these objectives will be achieved is presented in the following paragraphs. The measurement techniques and instrumentation used will be discussed in greater detail in the measurement section.

The first objective will be achieved by testing liquid fuels at room temperature in a laboratory environment. Infrared radiation from a blackbody source at a temperature similar to the effective radiation temperature in a fire [Kearney, 2001] will be transmitted through a small amount of liquid fuel and the spectral transmission of the radiation will be measured. Infrared spectral transmissivity information is available for a considerable number of compounds (for example, approximately 10,500 spectra are included in Pouchert [1985], and some 50,500 infrared spectra are available online from the National Institute of Advanced Industrial Sciences and Technology (Japan) at http://www.aist.go.jp/RIODB/SDBS/cgi-bin/cre_index.cgi). The thicknesses of the fluid layers are not always reported, however, and the majority of the available data neglects wavelengths smaller than 2.5 micron. Kearney [2001] found that emission from a large JP-8 fire approximated that of a gray body at about 1420 K, for which about 40% of the radiant energy is emitted at wavelengths shorter than 2.5 microns. Laboratory tests will be performed to measure the transmissivity of each of the liquid fuels used in this test series in the wavelength range of 1.3 to 4.8 microns, corresponding to the majority of the expected emitted radiation from the fire. The reflectivity of the liquid-air interface will be measured in six wavelength bands in the infrared range.

The second objective will be achieved by monitoring the rate of change of fuel mass with time for fires burning a number of different hydrocarbon fuel mixtures. A constant level system will be used to reduce transient effects due to the fuel level changing over the course of the test.

The third objective will be achieved by measuring the spectral radiation intensity from a fire over a very narrow view angle (0.25 degrees). A spectrometer will look upwards through a pipe which passes through the fuel pan. The spectrometer and pipe will be mounted below the pan on a positioning system that can move up and down to investigate the spectral absorption at various heights above the surface of the pool. A small number of viewing ports will be built into the fuel pan at different radial locations to study the variation with radial location in the pool.

The total heat flux at the surface of the fuel will be measured by heat flux gauges. The sensing surface of the gauges will extend a few millimeters above the surface of the pool. The surface-integrated heat flux to the pool will be obtained by integrating the measured heat fluxes across the pool surface. This total, integrated heat flux is believed to be the single most important factor in determining the fuel regression rate.

To meet the final objective small crushed glass pebbles will be placed within the liquid during some tests to restrict large scale motion within the pool. If this is found to change the fuel regression rate, the large scale convection will have been shown to be an important physical process in the actual fire that should be modeled for predictive fire simulations.

2. FACILITY, INSTRUMENTATION, AND PLANNED MEASUREMENTS

2.1 FRH Facility Description

The fuel regression rate experiments in liquid hydrocarbon fuels will be studied in controlled fire environments in the FLAME/Radiant Heat (FRH) test cell in the Thermal Test Complex (TTC) at Sandia National Laboratories (SNL). The main test chamber of the FRH cell is cylindrical in shape, 60 ft (18 m) inner diameter with a height around the perimeter of 40 ft (12 m). The ceiling slopes upwards (~18º) from the perimeter walls to a height of 48 ft (15 m) over the center of the facility. A round hole at the top of the facility 16 ft (4.9 m) diameter transitions to a 10 ft by 12 ft (3.0 m by 3.7 m) chimney duct (see Figure 1). The outer walls are made of steel channel sections and are filled with water that acts as a thermal sink during tests.

The ground level of FRH can be divided into three concentric sections. At the center of the facility is a fuel pan or gas burner. The facility can operate a gas burner (He, H_2, CH_4, etc.) or a liquid fuel pool (JP-8, methanol, etc.) up to 3 m in diameter. The test series discussed in this test plan will utilize a 2 m pool. The second section is a steel spill plate, which extends to a diameter of 6 m. The floor of the outer section is made of a steel grating, through which air is supplied to the FRH chamber during fire experiments. FRH is designed for flexibility in fuel types and a number of different fuels will be used in the present test series to evaluate spectral radiation fluxes to the fuel surface and regression rates for fuels of varying sooting propensities.

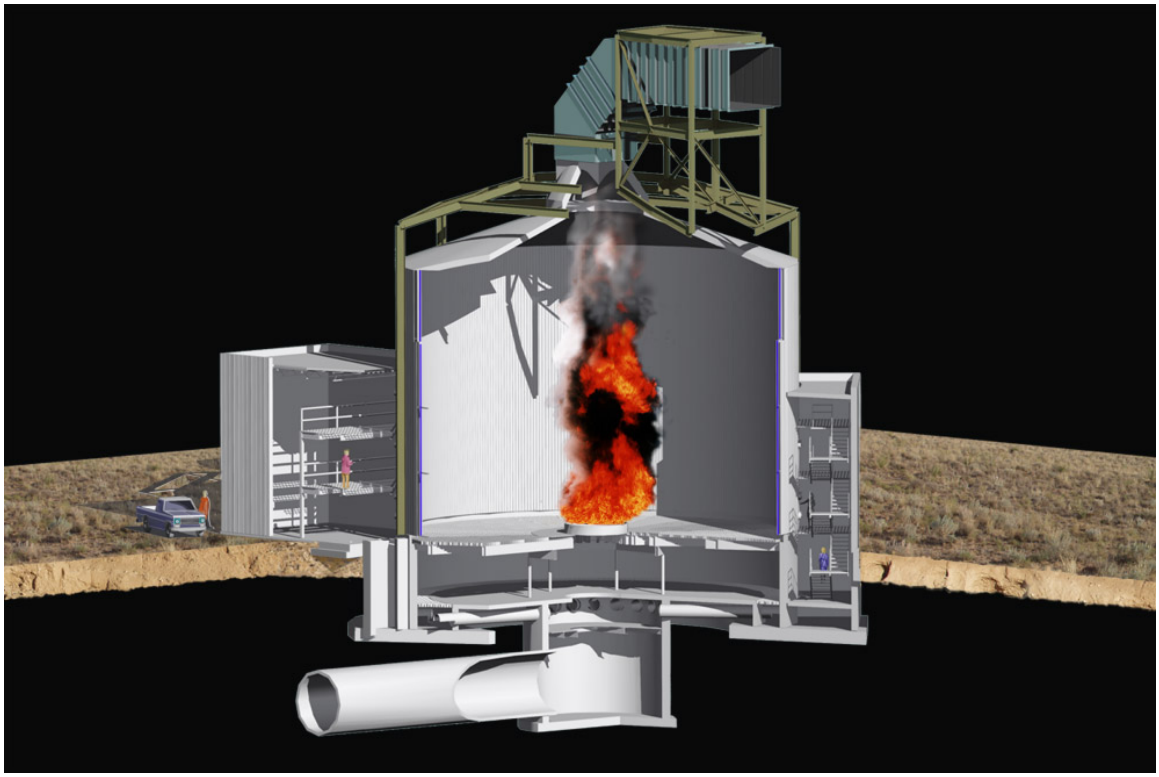

Figure 1 A cutaway view of the FRH facility showing a pool fire at the ground level, pipes supplying air flow through the basement, the chimney, and instrumentation rooms outside the FRH chamber.

The air flow in the FRH chamber combines contributions due to the buoyancy-controlled fire and due to the forced flow of air through the facility. The air flow in the absence of a fire has been characterized experimentally at the air ring in the basement and at the ground level (Ricks, 2006). The air ring flow field was found to exhibit a pattern (left side of Figure 2) attributable to the 18 supply pipes carrying the air from the diffuser in the center of the facility to the air ring along the outer edges of the facility (refer to Figure 1). The air flow at the ground level was found to be highest in the outer portion of the FRH cell, and exhibited a large recirculation zone in the inner portion of the facility, where mean velocities were in the negative (downward) direction (right side of Figure 2). The presence of a fire at the center of the facility is likely to reduce the recirculation because the air flow will be drawn inwards and entrained into the buoyant fire plume.

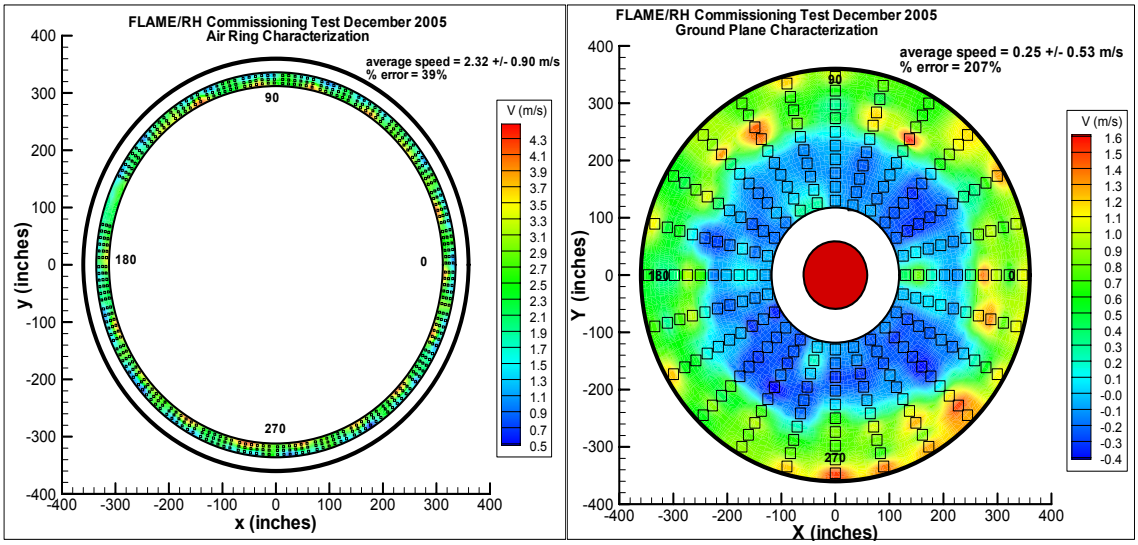

Figure 2 Measured mean velocities at the air ring in the basement of FRH (left) and at the ground level (right).

The test series discussed here will be performed with a liquid level control system to maintain a constant level of liquid fuel in the pan. Changes in the fuel level have been shown by Orloff and de Ris (1982) to influence the shape and burning characteristics of a fire, which they attributed to tripped turbulence at the lip of the pan. Maintaining a constant level is also important to prevent changes in radiation or convection interactions with the crushed glass in the fuel pan as the fuel level drops.

The liquid level control system is shown in Figure 3. Fuel is supplied to the pan from a standard 55 gallon drum located outside the FRH test chamber. The drum sits on a scale (Doran Model XL9000 with a customized 24 in. by 24 in. (61 cm by 61 cm) base to fit inside a spill pallet, manufactured by Doran Scales, Batavia IL). A positive displacement Alsco drum pump (model 2998 with 53 gpm (200 lpm) rated flow) draws fuel continuously out of the supply tank at a rate that is greater than the burning rate. The fuel that is not needed to maintain a constant amount of fuel in the pan is returned to the supply tank. The amount of fuel in the pan is inferred from differential pressure measurements made by a Rosemount Model 3051 differential pressure gauge and monitored by a Red Lion programmable controller. When the differential pressure measurement falls below the lower setpoint the controller opens a control valve (ASCO

EF8210B054 1 inch solenoid valve) allowing fuel to be fed to the pan through a ¾ in. (inner diameter) fuel rated hose. When the differential pressure reading reaches the upper setpoint the controller closes the control valve and the entire flow of fuel drawn out by the pump is simply returned to the supply tank. A second, identical Rosemount 3051 differential pressure gauge is used for data acquisition purposes. Differential pressure data are also obtained through the controller, but these data do not have the full resolution of the original differential pressure measurements.

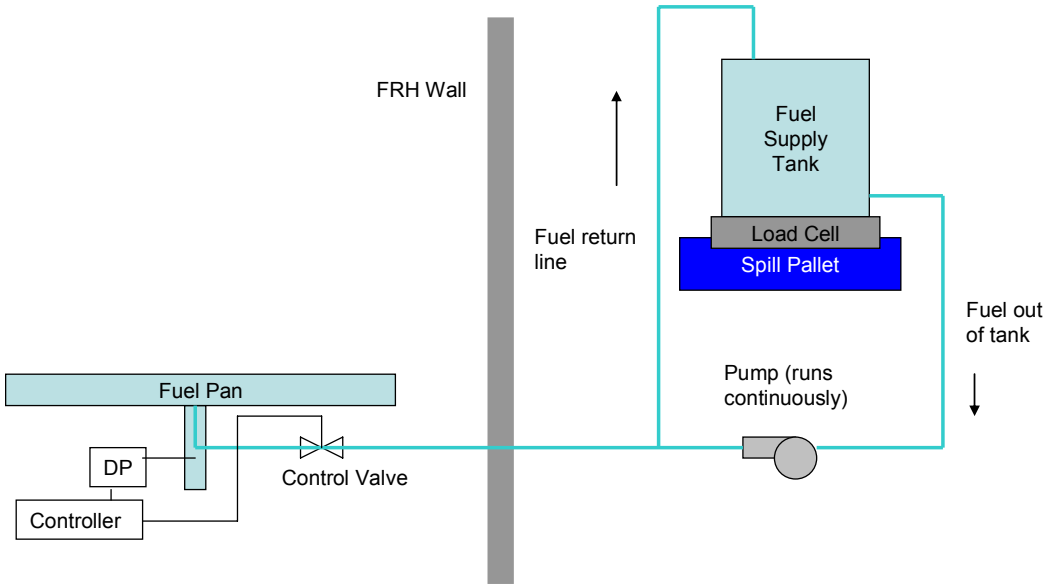

Figure 3 Schematic of the liquid level control system.

To minimize the disturbances to the differential pressure readings caused by the inflow of fuel into the pan, the fuel should not be discharged into the pan in close proximity to the gauge. For best stability the differential pressure gauges are mounted on the neck of the drain pipe beneath the fuel pan. The fuel is fed up through the neck and then through about 20 ft of perforated tubing to distribute the fuel inflow around the pan (not illustrated).

2.2 Principal Measurements

2.2.1 Fuel Regression Rates

Since fuel is supplied to the pan over the course of a fire test, the fuel regression rate will be determined from the rate at which fuel is drawn out of the supply tank. A scale (Doran Model 9000XL customized to fit on a spill pallet, Doran Scales, Batavia, IL) will measure the rate of fuel loss from the supply tank over the course of a test. The scale has a range of 0 to 500 lbs (0 to 227 kg) and a resolution of 0.05 lb (0.02 kg). The mass loss rate from the pool is found directly from the change in mass of the supply tank with time. The fuel regression rate is found from the mass loss rate, the area of the fuel pan, and the density of the fuel.

2.2.2 *Radiative Heat Transport to Pool*

The total heat transfer from the fire to the pool will be measured by an array of heat flux gauges (Model 64-20SB-18-5MGO-120-20970K Schmidt-Boelter type water-cooled thermopile gauges measuring total heat flux with a range of 0 to 120 kW/m^2, Medtherm Corporation, Huntsville, AL). The sensing surface of the gauges will be placed approximately 5 mm above the surface of the liquid fuel. The gauges will be placed at radial locations spaced such that each gauge is in the center of a concentric ring of equal area to minimize uncertainty in integrating the total heat flux over the surface of the pool (Figure 4). Duplicate gauges at the same radial distance from the pan center will be used to assess the degree of symmetry in the radial direction.

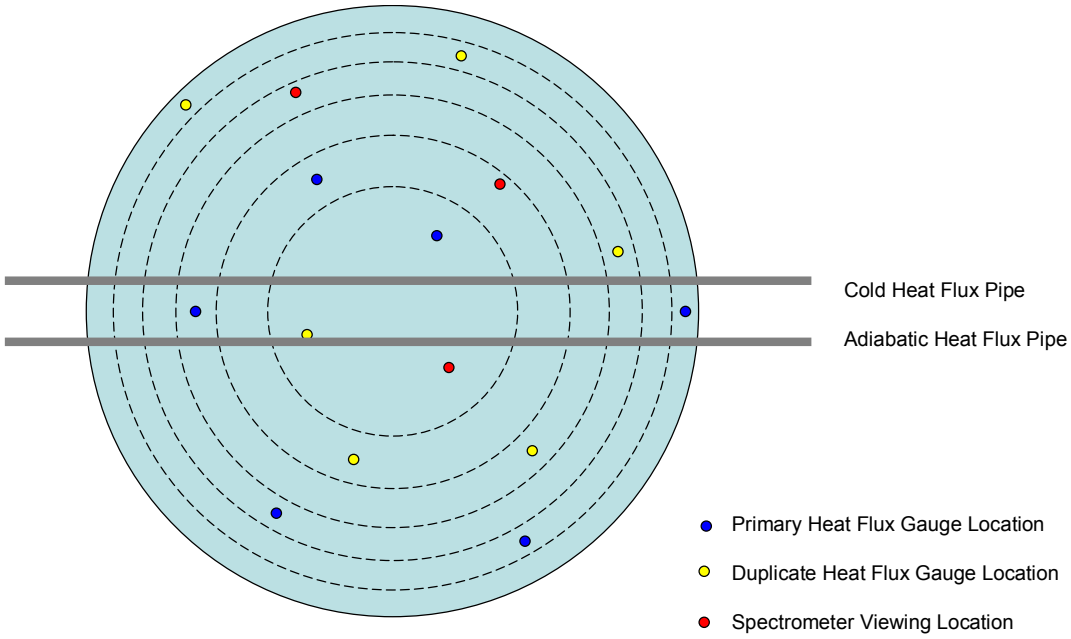

Figure 4 Proposed radial and angular locations of heat flux gauges and spectrometer viewing ports.

The effects of absorption of radiation by the gaseous fuel in the vapor dome will be studied in a subset of the fire tests in FRH. For these tests mid-infrared spectral radiation intensity measurements will be taken by an imaging spectrometer (model ES-200, Spectraline, Inc., West Lafayette, IN). The ES-200 measures spectral radiation intensity in the 1.3 to 4.8 micron wavelength range. This wavelength range accounts for 75% of the emitted radiation energy from a blackbody source at 1420 K, which is approximately the effective radiation temperature from a large hydrocarbon fuel fire as determined by Kearney (2001). The view angle of the spectrometer is approximately 0.25 degrees. The spectrometer will be mounted underneath the fuel pan, looking vertically upwards through a stainless steel pipe (1 in. diameter) which passes through a hole cut in the base of the pan (Figure 5). A small flow of nitrogen through the spectrometer and pipe will keep the optics clean and eliminate the contaminating effects of changes in gas composition within the pipe. The spectrometer and pipe will be mounted on a positioning system which traverses in the vertical direction to shift the viewing location from a height of 1 m above the pool surface down to the pool surface. The spectral intensity is expected

to decrease with decreasing height in the vapor dome due to absorption by the fuel vapor and soot.

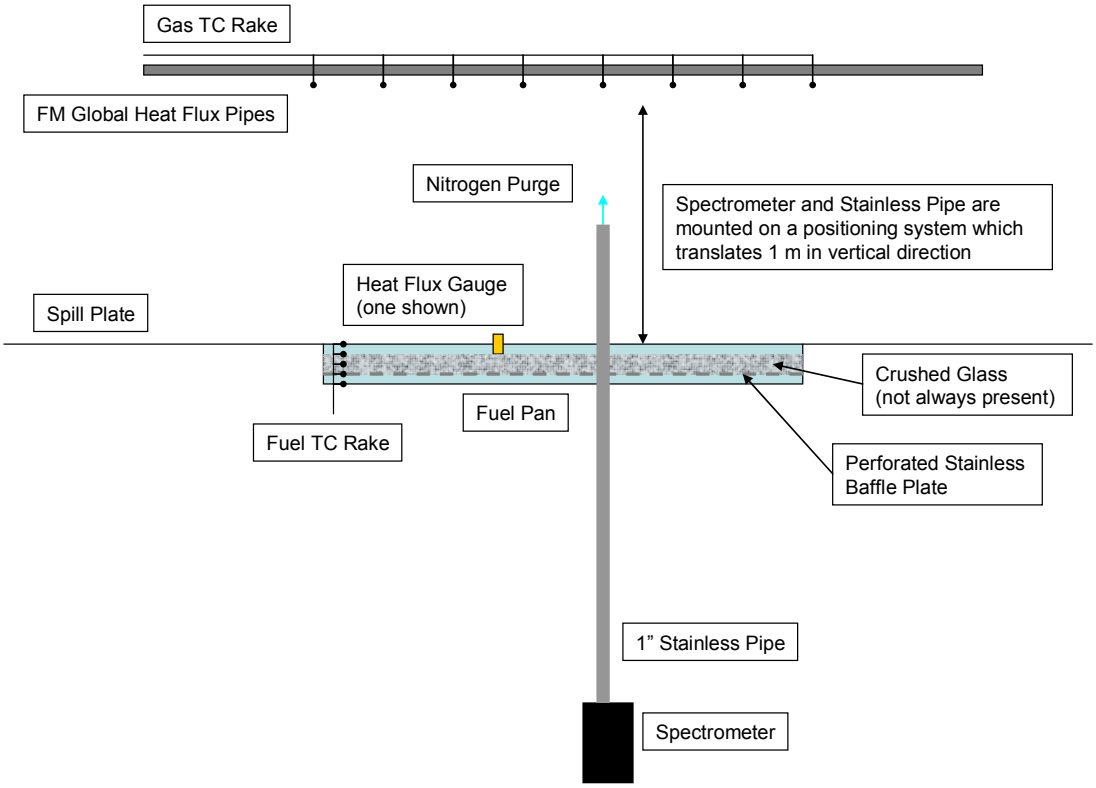

Figure 5 Schematic of instrumentation near pool for heat flux measurements.

2.2.3 Energy Transport in Liquid Fuel

The convective transport of energy in the liquid fuel will be tested by restricting the large scale motion of the fluid in some tests by introducing a bed of crushed glass in the liquid layer (refer to Figure 5). The crushed glass (opaque black irregularly-shaped pieces from 3 mm to 7 mm in size, Bourget Bros. Building Materials, Santa Monica, CA) will rest on a stainless steel screen (12-18 threads per inch) on top of the perforated stainless steel baffle plate in the pool. The depth of the pan is ¾ inch (19 mm) from the baffle plate to the surface of the pool, and the bed of crushed glass will begin approximately 3 mm below the surface. A rake of 40 mil (1.0 mm) MIMS type K thermocouples with a spacing of 10 per inch (2.5 mm spacing between thermocouples) will measure the temperature distribution across the depth of the pan. The magnitude of the differences in fuel evaporation rate between experiments with and without the crushed glass bed will provide a simple means of assessing the importance of convection within the liquid fuel.

The absorption of radiative heat flux to the surface will be assessed through reflectivity and transmissivity measurements for the liquid fuels which will be performed in the laboratory prior to the fire tests. Spectral transmission measurements for the liquid fuels to be burned in this test series will be taken using the ES-200 spectrometer described in the previous section. A liquid test cell containing a small amount of liquid fuel will be placed in front of the spectrometer,

which will look through the fuel at a blackbody source. The thickness of the liquid layer in the cell is adjustable from 0 to 4 mm with a resolution of 25 microns. Spectral absorption will be measured for all fuel mixtures at layer thicknesses of 1 mm and 4 mm. The available experimental data demonstrate that the spectral absorption in liquid hydrocarbon fuels is strongly wavelength dependent. In some spectral bands nearly all the energy is absorbed over a layer thickness of much less than a millimeter, but absorption in other bands may be small at millimeter thicknesses (see, for example, Dolphin and Wick [1977] pgs. 529, 533, and 539 where it is shown that there is >90% absorption over a significant fraction of the IR spectrum for methanol and ethanol in a liquid layer 25 microns in thickness but that the absorption is less than 10% over a significant fraction of the IR spectrum for toluene in a liquid layer of 100 micron thickness).

The reflectivity of the liquid fuel surface will be measured with an SOC 410 reflectometer (Surface Optics Corporation, San Diego, CA) in a laboratory environment prior to the fire tests. This handheld device measures the reflectivity of a surface at two different viewing angles in six wavelength bands, from which the total, hemispherical reflectivity may be estimated. The reflectivity measurements will be taken with a test setup designed to reliably position and align the reflectometer within 1 mm of the liquid surface.

These measurements will determine over what scale the radiation is important in the fuel and will provide guidance as to the level of detail that is required in the radiation treatment for a predictive fuel regression rate model.

2.3 Supplemental Measurements for Validation Studies

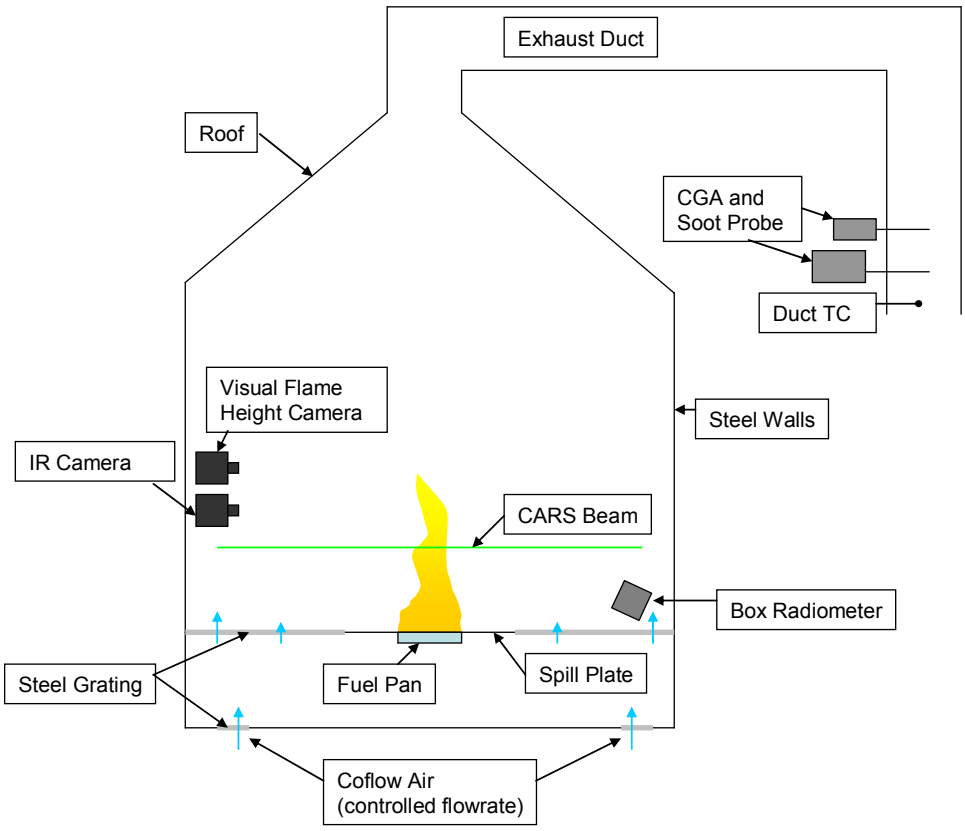

Figure 6 FRH cross section showing locations of instrumentation for supplemental measurements.

2.3.1 Air Flow Rate and Temperature

The coflow air supplied to FRH is controlled to maintain a constant flow rate at the desired value. A forced-draft fan forces air into the chamber at the specified flow rate. An induced-draft fan in the exhaust duct helps to draw air and combustion products out of the chamber and maintains the pressure at ambient levels. Both fans are computer controlled and the flow rate, fan speed, and current for each fan are logged. The air temperature is measured by a thermocouple in the basement of the FRH facility.

2.3.2 Wall Temperatures

The temperatures of the steel walls of the FRH chamber are measured by thermocouples mounted at heights of 1 ft (30 cm), 10 ft (3.04 m), 20 ft (6.08 m), 30 ft (9.12 m), and 39 ft (12.16 m) above the steel grating. The thermocouples are shielded from the radiation from the fire and the convective flow of the coflow air by a small piece of metal foil to minimize bias errors in the wall temperature measurement. These measurements are duplicated at four equally-spaced angular locations around the facility. The wall temperature measurements are of interest for imposed boundary conditions in validation simulations.

2.3.3 Radiative and Convective Heat Transfer to Objects within the Fire

Radiative and convective heat fluxes inside the fire will be assessed using two instrumented pipes, one water-cooled and one allowed to come to the temperature of the fire (refer to Figure 5). The methodology for separating convective and radiative heat fluxes has been described by de Ris [2004]. The rate of heat transfer to each pipe is measured by thermocouples embedded in the pipes. The ability to measure heat fluxes to the water-cooled pipe has been confirmed by Ricks [2006b]. The heat flux pipes will be placed at a height of 1 m above the fuel surface. The adiabatic and water-cooled pipes will be spaced a distance of 10 cm apart in the horizontal direction, each 5 cm from the center of the pool.

The convection measurements require the gas temperature outside the pipes. A rake of eight 1/16 in. MIMS type K thermocouples will provide temperature measurements in the vicinity of the heat flux pipes. The bias error in the thermocouple temperatures can be estimated from an energy balance for the thermocouple and the heat flux pipes and the thermocouple measurements corrected to the gas phase temperature [de Ris, 2004]. The thermocouple locations will be on the line equidistant between the two heat flux pipe axes, at distances of 6, 18, 30, and 42 inches (15, 46, 76, and 107 cm) to either side of the pool centerline. The support rod that the thermocouples are suspended from will be 30 cm higher than the heat flux pipes to minimize the effects of flame attachment on the measured heat fluxes.

2.3.4 Temperatures in the Fire

Temperatures inside the fire will be measured using coherent anti-Stokes Raman scattering (CARS) of the nitrogen molecule. CARS provides a point measurement of gas temperatures by a noninvasive, laser-based probing of the reacting flowfield. The details of the CARS process for probing sooting flames are provided by Kearney [2006]. Only a procedural summary the CARS measurements at FRH is provided here. Two pulsed laser beams are propagated into the FRH cell from the attached diagnostics laboratory. The laser beams are crossed at a common focus to form a CARS probe volume. The difference in wavelength between the two beams is tuned to drive the rotational-vibrational Raman transitions of nitrogen and a laser-like CARS signal is generated within the CARS probe volume. The CARS signal beam is forward propagated to a high-resolution grating-based spectrograph and the CARS signal spectrum is captured using a CCD camera. The spectral content of the CARS signal reveals how nitrogen population within the CARS probe volume is distributed among the allowed rotational and vibrational states and the gas temperature is determined from a best fit of theory to the experimentally obtained spectra.

CARS was successfully implemented in methanol fire tests in FRH under the C6 Radiation Partitioning experiments [Ricks et al. 2006 test plan, final report in preparation]. Gas temperatures in tests involving fuels with a greater sooting propensity may need to be estimated by other methods if the CARS signal is too greatly attenuated. The rake of thermocouples described in the previous section provides a second option for obtaining temperature data in the fire. The bias error in these temperature measurements can be estimated and corrected for, as described in the previous section.

2.3.5 Radiant Heat Flux to Objects outside the Fire

A wide-angle box radiometer custom built by FM Global (West Glocester, RI) will be used to measure the total radiation energy incident on an object some distance from the fire. A design sketch is shown in Figure 7. A commercial radiometer measures incident radiative heat flux. The box enclosure in front of the radiometer restricts the field of view to a user-adjustable view angle in the vertical and horizontal directions to eliminate radiation contributions from sources other than the fire. A shutter can be closed periodically to check for drift in the measurements by comparing against a cold dark background. The box radiometer will be positioned at the level of the base of the flame, 8.5 m from the center of the burner, with a 35.2º view angle to capture the radiation from the fire over its entire height.

2.3.6 Average Flame Height

The average flame height will be determined from visual data from a video camera in the FRH test cell. Prior to the test each position within the camera frame will be mapped to a height above the centerline of the fire using a stadia board. The flame height will be assumed to be the height at the centerline corresponding to the location within the camera frame in which the flame is visible at least 10% of the time. Both a visual and an IR camera will be employed for comparison.

2.3.7 Composition of Combustion Products in Overfire Region

The composition of the combustion products above the fire will be monitored using a Combustion Gas Analyzer (CGA) in the chimney. The CGA (Land Instruments International, model FGA II) measures the concentrations of CO, CO_2, O_2, NO, NO_2, NO_x, and SO_2. Laser extinction measurements similar to those taken at the old FLAME facility [Jensen and Brown, 2004] are taken near the CGA and provide an estimate of the soot concentration, further extending the knowledge of the combustion products in the over-fire region. The temperature of the exhaust gases is measured by a thermocouple close to the soot probe and CGA locations in the exhaust duct.

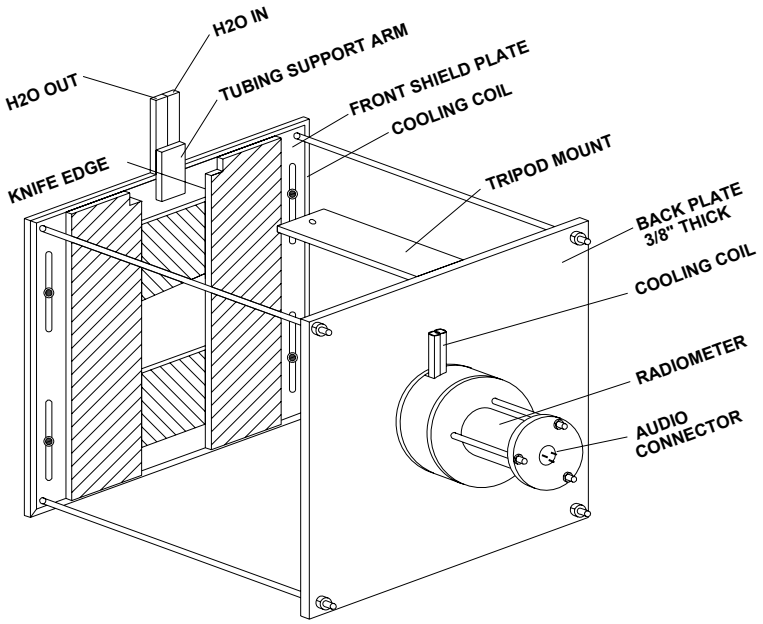

Figure 7 Design sketch of wide-angle radiometer.

3. DESIGN OF EXPERIMENTS

A number of fuels and fuel mixtures have been selected for study in this test series. The assistance of John de Ris and Patricia Beaulieu in selecting the fuel mixtures is gratefully acknowledged (Beaulieu [2005]). All fuel mixtures will be tested for their transmittance and reflectance in the laboratory prior to the fire experiments. A summary of fuel mixtures, convection restrictions, and pan diameters for each test is given in

Table 1 . Tests 1 through 5 were selected to maintain a constant sooting propensity as determined from their smoke point. The sooting propensity is potentially an important parameter because soot is the primary source (and sink) of radiation in typical hydrocarbon fires. Test 2 and Tests 6 through 11 use the same mixture of fuels while varying the smoke point. These tests maintain the heat of gasification relatively constant. The heat of gasification is a potentially important parameter because it controls the energy that must be absorbed to vaporize the liquid fuel. Tests 12 through 17 cover a range of other mixtures with different smoke points and heats of gasification to fill in the parameter space. Five of the fuel mixtures were selected for the study of convection effects by restricting large scale motion in the pool. These tests were chosen to cover much of the parameter space for heat of gasification and sooting propensity.

Table 1 Test Matrix for Fuel Regression Rate Tests

Test Number	Fuel A (%vol)	Fuel B (%vol)	Crushed Glass?	Pan Diameter (m)
1	heptane (98%)	toluene (2%)	no	2
2	acetone (97%)	toluene (3%)	no	2
2-a	acetone (97%)	toluene (3%)	yes	2
3	ethyl alcohol (56%)	isooctane (44%)	no	2
4	ethyl alcohol (84%)	toluene (16%)	no	2
5	methyl alcohol (76%)	toluene (24%)	no	2
5-a	methyl alcohol (76%)	toluene (24%)	yes	2
6	heptane (100%)	toluene (0%)	no	2
7	heptane (90%)	toluene (10%)	no	2
7-a	heptane (90%)	toluene (10%)	yes	2
8	heptane (80%)	toluene (20%)	no	2
9	heptane (70%)	toluene (30%)	no	2
10	heptane (50%)	toluene (50%)	no	2
10-a	heptane (50%)	toluene (50%)	yes	2
11	heptane (0%)	toluene (100%)	no	2
12	ethyl alcohol (70%)	isooctane (30%)	no	2
13	methyl alcohol (50%)	toluene (50%)	no	2
14	acetone (86%)	isooctane (14%)	no	2
15	ethyl alcohol (90%)	toluene (10%)	no	2

Test Number	Fuel A (%vol)	Fuel B (%vol)	Crushed Glass?	Pan Diameter (m)
16	ethyl alcohol (70%)	toluene (30%)	no	2
17	JP-8 (100%)	-	no	2
17-a	JP-8 (100%)	-	yes	2

In order to reduce cost and meet schedule requirements, a reduced test matrix (to be supplemented with pure methanol, heptane, and possibly toluene will be performed). Figures 8 and 9 show that the reduced test matrix will provide the data required to populate the parameter space of heat of gasification versus smoke point. Table 3 presents properties of the base component fuels.

Table 2 Reduced Test Matrix

Test Number	Fuel A (%vol)	Fuel B (%vol)	Crushed Glass?	Pan Diameter (m)
1	heptane (98%)	toluene (2%)	no	2
1-a	heptane (98%)	toluene (2%)	yes	2
2	ethyl alcohol (56%)	isooctane (44%)	no	2
3	methyl alcohol (76%)	toluene (24%)	no	2
3-a	methyl alcohol (76%)	toluene (24%)	yes	2
4	heptane (80%)	toluene (20%)	no	2
5	heptane (50%)	toluene (50%)	no	2
5-a	heptane (50%)	toluene (50%)	yes	2
6	methyl alcohol (50%)	toluene (50%)	no	2
7	ethyl alcohol (90%)	toluene (10%)	no	2
8	JP-8 (100%)	-	no	2
8-a	JP-8 (100%)	-	yes	2

Table 3 Properties of Selected Fuels

Fuel Name	MW	Boiling Point	Smoke Point	Heat of Vaporization	Specific Heat	Heat of Gasification	Density
		(°C)	(m)	(kJ/kg)	(kJ/kg K)	(kJ/kg)	(g/cm3)
heptane	100.2	99	0.120	364.9	2.25	541	0.684
acetone	58.1	56	0.205	523.0	2.18	601	0.789
ethyl alcohol	46.1	78	-	837.0	2.44	978	0.789
methyl alcohol	32.1	64	-	1100.9	2.53	1211	0.791
toluene	92.2	110	0.005	362.8	1.70	515	0.866
isooctane	114.0	125	0.080	301.8	2.23	527	0.698
JP 8	-	300	0.025	250	2.4	922	0.800

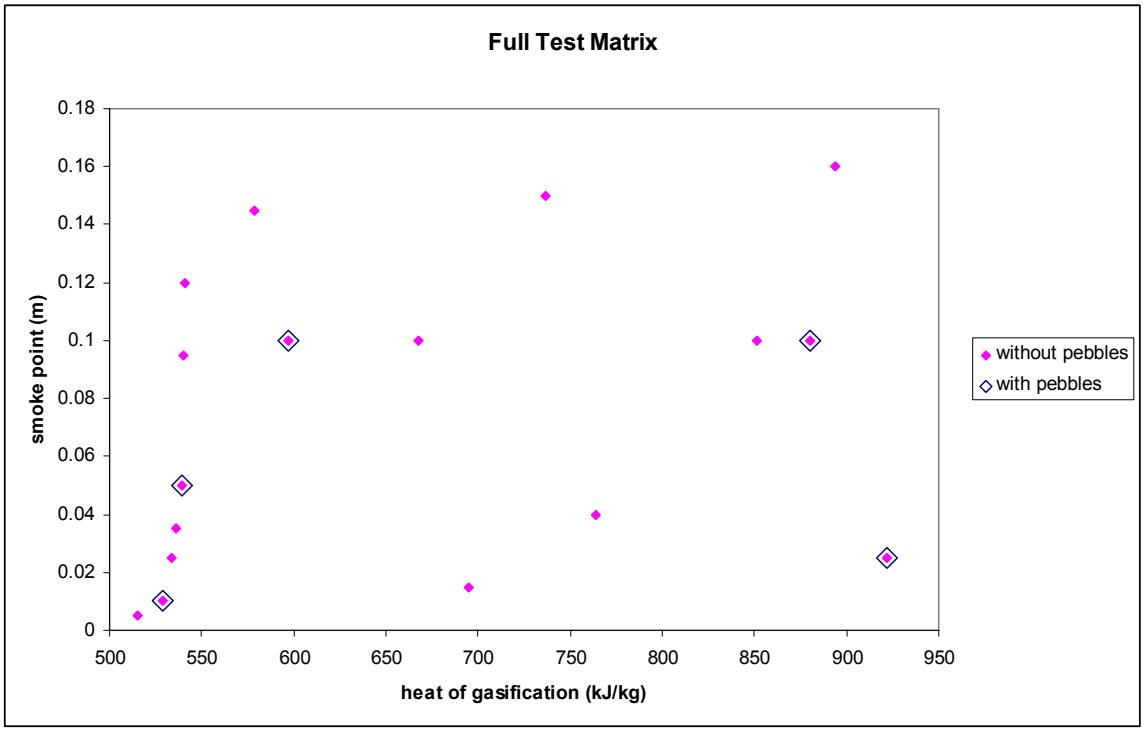

Figure 8 Full test matrix mapping.

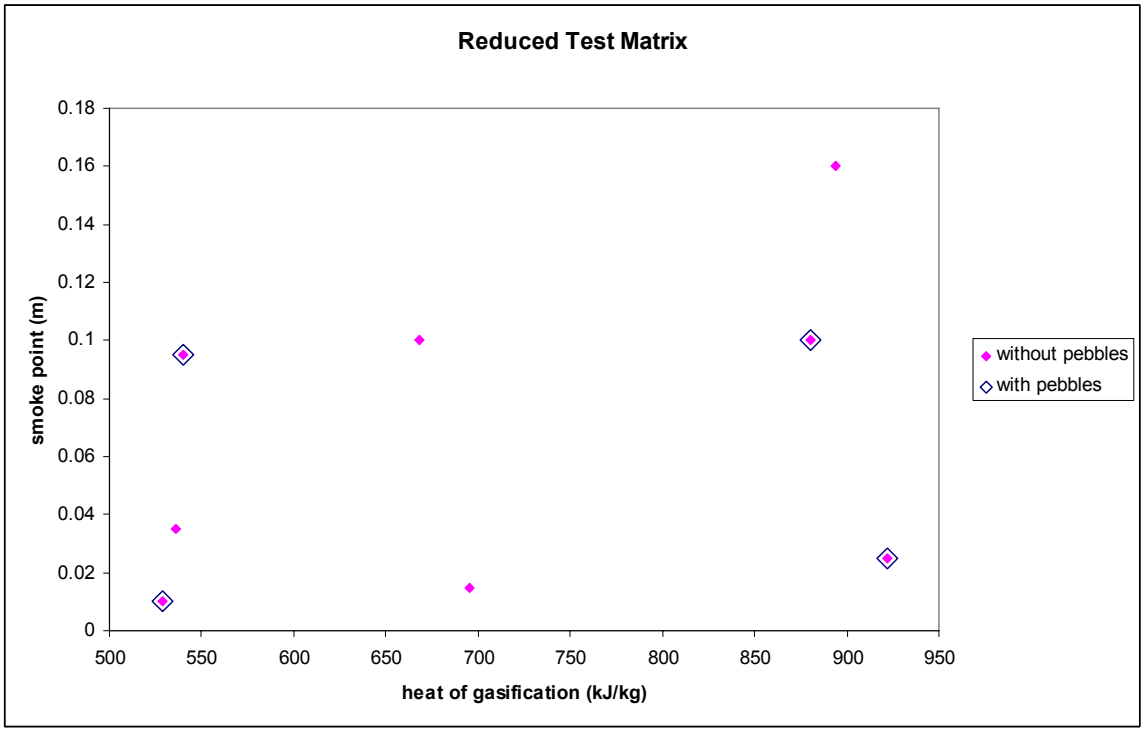

Figure 9 Reduced test matrix mapping.

3.1 Test Procedures

The fire will be ignited with a propane igniter and allowed to burn for approximately 5 minutes before taking spectal radiation data to avoid the initial transient phase of the fire. Data from all instruments except the spectrometer will be taken continuously at fixed locations throughout the test. The spectrometer viewing position will be changed several times throughout the course of a test, with enough data acquired at each location to obtain time-averaged results. Filling of the pool to maintain a constant fuel level will be performed automatically throughout the test and the amount of fuel added will be monitored. Mean fuel regression rates are found from the time-averaged filling rates.

3.2 Data Acquisition

The data acquisition system (DAS) consists of a PC with a 16-bit data acquisition card connected to a National Instruments (NI) SCXI-1001 chassis. It has twelve NI SCXI-1102 cards with NI SCXI-1303 blocks for TCs and four NI SCXI-1104 cards with NI SCXI-1300 blocks for analog signals. This provides the ability to increase either analog signals or TC signals. Note that the SCXI-1001 presently holds 12 cards, yielding a total channel count of 384 channels if all slots are used for data acquisition. The system is upgradeable simply by adding an additional SCXI-1001 DAQ card and more multiplexer units (MUXs).

The data acquisition system can acquire temperature, heat flux, and pressure data. The integrity of all thermocouple channels is evaluated prior to each experiment with an Ectron thermocouple simulator, which inputs a controlled signal into each channel at the thermocouple device connection point and provides a check on the integrity of the channel hardware and software from that point to the final magnetic storage location.

Data are sampled simultaneously for all channels, typically at 1000 Hz with an average value recorded at a rate of at least one sample per second, starting at least two minutes prior to the fuel ignition and continuing after burnout of the fire.

A formal checklist for conducting the test is created and used to record actions during the test event. The data from the instrumentation are organized via a Data Channel Summary Sheet and with sketches showing instrumentation location. This summary sheet contains a channel-by-channel listing of the instrumentation with details such as expected range, sampling rate, calibration date and source, instrument location, and the data sample rate. Post-test, all data are collected and converted to electronic format for purposes of archiving and dissemination via PC media (i.e., CD or equivalent).

3.3 Uncertainty Analysis

An uncertainty analysis for all measurements will be performed. The methodology follows Coleman and Steele [1999]. Bias errors which can be mathematically modeled, such as the bias error in thermocouple measurements in the fire, are algebraically added to the measurement and the uncertainty in the estimation of the bias is treated as a random error [Romero et al., 2005].

3.3.1 Fuel Regression Rates

In the present experiments the fuel regression is determined from the rate of change of mass of a fuel supply tank (previously described). The constant-level control system matches the averaged rate of mass loss from the supply tank to the averaged mass loss rate from the pool, but fuel is supplied to the pan at a rate greater than the regression rate when the control valve is open and is not supplied to the pan when the control valve is closed. The nature of the control system dictates that fuel regression measurements should be averaged over periods much larger than the typical cycle time between commanded signals to open the control valve. A cycling rate of about 2.9 cycles per minute was observed in methanol tests that were run during development of the constant level system.

The scale used for measuring the rate of change of fuel mass during the course of a test is resolved to 0.05 lb (0.02 kg) with an uncertainty of ±0.06 kg. Uncertainty in the averaged fuel regression rate decreases as a function of the time over which the results are averaged. For a 2 m pool of methanol, density 0.789 kg/m^3, with a fuel regression rate of 1.2 mm/min the total mass loss from the fuel over a 10 minute span is 29.7 kg. Since fuel is not supplied to the pan continuously, the uncertainty in the actual amount of fuel added to the pan will be assumed to be half the average mass added per cycle. If the fuel fill cycle rate is 2.9 cycles per minute, the uncertainty due to the unsteady fill rate is ±0.51 kg. If the uncertainty in the pan area, fuel density, and time between measurements are neglected, the total RSS combined uncertainty in the fuel regression rate measurement is ±0.02 mm/min or 1.7%.

3.3.2 Total Heat Flux to Fuel Surface

The manufacturer's stated uncertainty for the heat flux gauges used to measure the incident heat flux at the pool surface is ±3%. Nakos [2005] estimated that uncertainties in fire applications can be much larger (±20% to ±40%), largely due to uncertainties in the convective component of heat transfer. The uncertainty in the measurement of heat flux to the fuel includes the gauge measurement uncertainty, the uncertainty in the net heat flux due to differences in temperature and reflectivity between the fuel and the gauge, and the uncertainty in the integration of heat flux over the pool surface area based on measured heat fluxes at a finite number of measurement locations. For the present work the temperature within the liquid fuel will be measured by a rake of thermocouples, but the temperature at the surface will be assumed to be the temperature of a saturated mixture at ambient pressure. The temperature of the heat flux gauge will be assumed to be that of the cooling water supplied to the gauge. The reflectivity of the liquid fuel will be measured in the laboratory and the reflectivity of the heat flux gauge will be assumed to be one minus the manufacturer's stated absorptivity. The sensitivity to the limited number of data points will be assessed by installing additional heat flux gauges at duplicate radial locations and comparing the measured heat flux based on each of the duplicate gauges. This also provides a means of estimating the uncertainty due to the assumption of axisymmetry. The sensitivity to limited data points in the radial dimension will be assessed by computing the total heat transfer in two ways. For the first method the pool surface area is divided into concentric rings of equal area within each of which a heat flux gauge is located. The total heat flux is calculated as the average of the heat flux gauge measurements, which is equivalent to assuming that the heat flux is constant across each ring at the value measured by the heat flux gauge. For the second method a continuous curve will be constructed which approximates the measured distribution of heat

flux with radial position. The total heat transfer is computed from the analytic integral of the continuous curve. Final evaluation of the uncertainty will be performed post-test.

3.3.3 Spectral Transmission Coefficients in Fuel Vapor in Fires

The manufacturer's stated uncertainty for the Spectraline ES-200 spectrometer is ±0.5% of full range of the signal (0 to 10 Volts), which corresponds to the random error in the measurement. The accuracy of the intensity or the transmission coefficient measurement is then a function of the accuracy and appropriateness of the calibration. For transmission measurements the average voltage measured at the top of the vapor dome is used as a reference, and the ratio of the measured voltage lower in the vapor dome to the reference voltage is taken to be the transmissivity. With a baseline intensity appropriate for a fire, the maximum and minimum reference voltages are estimated for the present analysis to be 1.5 V and 0.5 V. The uncertainty in the transmissivity due to the random error in the recorded voltage is then ±0.03 transmissivity units at the maximum intensity and ±0.10 transmissivity units at the minimum intensity. If the uncertainty in the reference voltage is assumed to be ±15%, the overall uncertainties rise to ±0.15 and ±0.18 transmissivity units.

3.3.4 Spectral Transmission Coefficients in Liquid Fuels

The same spectrometer is used for spectral transmission in the liquid fuel as in the fuel vapor. The absorption of the liquid test cell without any fuel in it can be measured independently in a steady environment, reducing the uncertainty in the determination of the reference voltage as compared to the study of the absorption in the vapor dome. If a blackbody source at 1200ºC is assumed to provide the spectral energy, the maximum and minimum voltages are assumed to be 6.5 V and 0.3 V. The uncertainty due to the random error in the voltage measurement then ranges from ±0.01 to ±0.17 transmissivity units. If the uncertainty in the reference voltage is assumed to be ±5%, the overall uncertainties rise to ±0.05 transmissivity units at the maximum intensity and ±0.17 transmissivity units at the minimum.

3.3.5 Reflectivity of Liquid Fuel

The uncertainty of the reflectivity measurements taken by the SOC 410 is ±0.03 reflectivity units for temperatures in the range 0ºC to 40ºC. The measurement applies to the interface between the liquid fuel and air at room temperature. The reflectivity of the interface between the liquid fuel and the gaseous mixture in the actual fire will be assumed to be similar, so the overall uncertainty in the reflectivity will be assumed to be ±0.05 reflectivity units.

3.3.6 Temperature of Liquid Fuel

An uncertainty analysis for thermocouple data acquisition systems in use at Sandia's Radiant Heat facility and the Lurance Canyon burn site has been performed by Nakos [2004]. The analyses apply to Type K, chromel-alumel thermocouples in MIMS thermocouple assemblies and other applications. Several DASs were analyzed, one Hewlett-Packard (HP) 3852A system, and several NI systems. The uncertainty analyses were performed on the entire system from the thermocouple to the DAS output file. Uncertainty sources include thermocouple mounting errors, ANSI standard calibration uncertainty for Type K thermocouple wire, potential errors due to temperature gradients inside connectors, extension wire effects, DAS hardware uncertainties

including noise, common mode rejection ratio, digital voltmeter accuracy, mV to temperature conversion, analog to digital conversion, and other possible sources. Typical results for "normal" environments (e.g., maximum of 300 to 400 K) showed the total uncertainty to be about ±1% of the reading in absolute temperature. In high temperature or high heat flux ("abnormal") thermal environments, total uncertainties range up to ±2-3% of the reading (maximum of 1300 K). The higher uncertainties in abnormal thermal environments are caused by increased errors due to the effects of imperfect thermocouple attachment to the test item.

The ANSI standard uncertainty for Type K thermocouple wire is 2.2ºC or 0.75% of reading (in ºC), whichever is greater. This uncertainty applies to the temperature of the thermocouple junction itself. Determination of the actual desired temperature (wall temperatures of an object or fluid temperatures) is subject to additional bias errors due to mounting. These bias uncertainties are very hard to accurately quantify, are application dependent, and are often the largest errors in the measurement system. For the present tests the bias error in the liquid fuel measurements will be assumed to be small compared to the thermocouple uncertainty. The thermocouple is in good thermal contact with the liquid, which has a thermal conductivity much greater than that of air. Furthermore, radiation errors, etc. are expected to be small within the liquid. The local liquid temperature is expected to vary slowly compared to the thermal response time of the thermocouple. The overall uncertainty of the liquid fuel temperatures will be assumed to be ±3ºC, which adds some conservatism to the ANSI standard uncertainty over the range of temperatures at which the fuel is expected to exist in liquid form.

3.3.7 Air Flow Rate and Temperature

The air flow rate is measured by a Veltron II pressure and flow transmitter (Air Monitor Corporation, Santa Rosa, CA). The Veltron II calculates the air velocity and flow rate based on a differential pressure measurement. The differential pressure is measured to an accuracy of 0.1% of the natural span of the transmitter (10 inches of water). The uncertainty in the velocity due to the differential pressure uncertainty is approximately ±3% at the chosen flow rate of 150,000 scfm. When the uncertainties due to non-uniformity in the velocity profile, tolerances on the duct dimensions, etc. are included the total uncertainty is estimated to be approximately ±6% of the total flow rate.

Air temperature measurements are performed by thermocouples similar to those used in the liquid fuel measurements. The air temperature measurements are made inside a duct in a relatively cool environment in which convective heat transfer from the air to the thermocouple is expected to dominate, therefore the uncertainty in the air temperature will be assumed to be the same as the uncertainty in the fuel temperature measurements, ±3ºC.

3.3.8 Wall Temperatures

Wall temperature measurements are made by thermocouples mounted to the steel walls of the FRH chamber. The thermocouples are in good thermal contact with the walls, which have a very high thermal conductivity. The thermocouples will be partially shielded from the radiation of the fire and convection from the cool coflowing air. Previous experience has shown that the walls remain relatively cool during tests due to their large thermal mass. The analysis of Nakos [2004]

suggests that the maximum error is ±1% of the reading (in K) for temperatures up to 400K. An uncertainty of ±4ºC will be assumed for the wall temperatures in the present tests.

3.3.9 Convection and Radiation inside the Fire

Convection and radiation measurements inside the fire will be made using a combination of hot and cold heat flux pipes (previously described). Ricks [2006b] performed calibration experiments to assess the ability of the cold heat flux pipes to predict the heat transfer by radiation in a controlled environment. The heat flux measurements calculated based on the apparent heat flux to the pipe were in excellent agreement with the estimated incident radiative heat flux based on a radiation exchange analysis. The emissivity of the pipe was shown to be a significant contributor to the uncertainty in the absorbed radiation. The physical spacing of thermocouples and the finite time response of the heat flux pipe were shown to limit the ability to resolve spatial or temporal variations in heat flux.

In the rapidly fluctuating environment of a fire the smallest length and time scales over which heat flux varies will not be resolved by the heat flux pipes. The heat flux can be spatially resolved to 12 in. (30 cm) increments for the pipes used in the present experiments. Ricks [2006b] showed that the temporal resolution is approximately 10 seconds at cooling water flow rates appropriate for the heat flux pipe in a fire environment. Uncertainty in individual thermocouple measurements are assumed to be the same as for the liquid fuel measurements; however the heat fluxes are based on differential temperature changes rather than absolute temperature values, and these values are seen to change very little (fluctuations of no more than ±0.1K about mean values for each thermocouple). The error in the temperature difference between two adjacent thermocouples is assumed to be no greater than ±1K once the bias error for each thermocouple has been removed. The expected uncertainty in spatially and temporally filtered heat flux is expected to be ±7.0 kW/m^2 at cooling water flow rates appropriate for a fire, which is roughly 5% of the expected total heat flux.

The adiabatic pipe, like the water-cooled pipe, provides temporally and spatially filtered heat flux data. The spatial filter for the adiabatic pipe is the same as for the water-cooled pipe. The temporal filter is expected to be somewhat longer because the adiabatic pipe must come up to the temperature of its surroundings. In contrast to the water-cooled pipe, the determination of the heat flux does not depend upon spatial temperature gradients in the pipe because there is no energy transport by cooling water flow in the adiabatic pipe. If errors in the time rate of change of temperature are assumed to be no greater than ±0.5K/s over temporally resolved scales and the uncertainty in the determination of the heat capacity of the adiabatic pipe is assumed to be 5%, uncertainty in the spatially and temporally filtered heat fluxes is approximately 7.5% at heat flux values expected in the fire.

With equations for the heat transfer to the adiabatic pipe, cold pipe, thermocouple, and with appropriate correlations for the convection heat transfer coefficient for each, it is possible to solve for the gas phase temperature and the incident radiation heat flux. The analysis actually provides more equations than unknowns, so the option exists to solve the equations in several different ways. Further analysis is required to determine which method predicts the incident radiative flux and the convection to each object with the lowest uncertainty.

3.3.10 Temperatures inside the Fire

Two methods will be employed to measure temperatures inside the fire. The first method is to use thermocouples with a correction technique [de Ris, 2004]. Ricks et al. [2006 test plan, final report in preparation] evaluated a similar correction technique employing two type K MIMS thermocouples of different sizes [Brohez et al., 2004] but estimated that the uncertainty in the correction factor was greater than 100% even in relatively steady, well controlled environments. In previous tests the uncertainty in corrected local gas temperatures in the open-ended annulus between a heated cylindrical shroud and calorimeter was estimated to be as large as ±300K [Ricks et al. 2006 test plan, final report in preparation]. The uncertainty depends strongly on the local velocity and radiation fields. A full uncertainty analysis will be performed post-test to assess the uncertainty in this application, however the expected uncertainty in local temperatures averaged over a span of at least 10 seconds will be assumed to be comparable to the uncertainty found by Ricks et al. [2006 test plan, final report in preparation].

The second measurement technique for measuring gas temperatures inside the fire is CARS. Typical uncertainties in single-laser-pulse CARS temperature measurements in laboratory flames range from 3-5%, with some reduction in uncertainty when the CARS spectrum is averaged over many laser pulses. Kearney and Grasser [2007] estimated that the single-shot CARS measurements taken with the instrumentation system developed for use in FRH have an uncertainty of 6.8%. Uncertainties in temperature measurements for the fires in this test series can be expected to be somewhat larger due to the greater sooting propensity of the fuel mixtures in this test series.

3.3.11 Incident Radiation on Objects outside the Fire

The incident radiative heat fluxes to objects outside the fire are measured by a custom built box radiometer. The box radiometer was calibrated after assembly by the manufacturer. The uncertainty in the measurement is the total uncertainty in the radiometer calibration. A typical radiative heat flux calibration uncertainty of ±3% will be assumed.

3.3.12 Average Flame Height

The flame height is defined herein as the highest point at which a flame is visible at least 10% of the time. Images will be recorded on video from both a visual and an IR camera for comparison. Uncertainty in the actual height of the visible flame in an individual image is estimated to be approximately 10 cm. Uncertainty in determination of the average flame height based on a minimum of 1000 video frames will be assumed to be equal to the uncertainty in determining the height of the flame within the frame.

3.3.13 Combustion Products Composition

The CGA resolves the concentrations of minor species CO, NO, NO_2, SO_2 to 0.1 ppm. Concentration of CO_2 is resolved to 1000 ppm and O_2 is resolved to 100 ppm. Uncertainties for all species except O_2 are a function of the user-specified total range for that species. The uncertainties are given as ±2% of the range for the calibration linearity, with additional components for zero drift and span drift over time. The uncertainty due to calibration is a fixed ±2000 ppm for O_2. The drift contributions become comparable to the linearity contributions

after approximately one month between calibrations. For the present work the overall uncertainties will be assumed to be ±3000 ppm for O_2 and ±3% of the full range for each of the remaining species.

Jensen and Brown [2004] estimated the total uncertainty in soot yield fraction for a soot probe similar to the one used in the present test series to be ±26.0% of the measurement. The largest single contributor to the uncertainty was the uncertainty in the fuel regression rates, which was limited by low resolution in the regression measurements of ±0.5 mm/min (~20%) in their application. As previously discussed, uncertainty in fuel regression rates for the present test series will decrease as the averaging time increases and become small (~2%) over ten minute intervals. The total uncertainty in the present experiments based on an uncertainty of ±5% in the fuel regression rate but otherwise with the same uncertainties as reported by Jensen and Brown [2004], is ±17.4% of the measurement.

Temperatures in the exhaust duct are measured by a thermocouple located near the CGA and soot probe. At this location the flow can be assumed to be relatively uniform and to vary slowly compared to the time response of the thermocouple. Furthermore, the heat transfer is expected to be dominated by convection due to the large flow rate and the assumed uniformity in temperatures throughout the duct. The uncertainty of temperature measurements in the duct is assumed to be the same as the uncertainty of the coflow air temperature measurements.

4. REFERENCES

Babrauskas, V., "Estimating large pool fire burning rates," *Fire Technology* 19:251-261, 1983.

Beaulieu, P., FM Global Research, Informal communication to Tom Blanchat, Sandia National Laboratories, May 2005.

Brohez, S., Delvosalle, C., and Marlair, G., "A two-thermocouples probe for radiation corrections of measured temperatures in compartment fires," *Fire Safety Journal*, Vol. 39, 399-411, 2004.

Brown, A. L., Gill, W., and Lopez, C., "Predictive evolution of fuel from a liquid pool fire: phenomenology identification and ranking exercise," paper IMECE2006-15157, *Proceedings of International Mechanical Engineering Congress and Exposition*, November 5-10, 2006, Chicago, IL.

Chatris, J. M., Quintely, J., Folch, J., Planas, E., Arnaldos, J., and Casal, J., "Experimental study of burning rate in hydrocarbon pool fires," *Combust. Flame* 126:1373-1383, 2001.

Coleman and Steele. *Experimentation and Uncertainty Analysis for Engineers*, Wiley & Sons, 1999.

de Ris, J., FM Global Research, Informal communication to Tom Blanchat, Sandia National Laboratories, December, 2004.

Dolphin, D., and Wick, A. E., *Tabulation of infrared spectral data*, Wiley-Interscience, John Wiley and Sons, New York, NY, 1977.

Hottel, H. C., "Certain laws governing diffusive burning of liquids," *Fire Research Abstracts Reviews* 1:41-43, 1959.

Jensen, K. A., and Brown, A. L., "Measurement of soot yield from JP-8 pool fires using light extinction," INTERFLAM04, Edinburgh, Scotland, July 5-7, 2004.

Kearney, S. P., "Temporally resolved radiation spectra from a sooting, turbulent pool fire," *Proceedings of International Mechanical Engineering Congress and Exposition*, November 11-16, 2001, New York, NY.

Kearney, S. P., and Jackson, M. N., "Dual-pump CARS thermometry in sooting acetylene-fueled flames," 44th AIAA Aerospace Sciences Meeting and Exhibit, 9-12 Jan., 2006, Reno, NV.

Kearney, S. P., and Grasser, T. W., "CARS thermometry in a 2-m-diameter methanol pool fire," 45th AIAA Aerospace Sciences Meeting and Exhibit, 8-11 Jan., 2007, Reno, NV.

Koseki, H., "Combustion properties of large liquid pool fires," *Fire Technology* 25(3):241-251, 1989.

Koseki, H., and Mulholland, G. W., "The effect of diameter on the burning of crude oil pool fires," *Fire Technology* 27(1):54-65, 1991.

Koseki, H., and Iwata, Y., "Tomakomai large scale crude oil fire experiments," *Fire Technology* 36(1):24-38, 2000.

Muñoz, M., Arnaldos, J., Casal, J., and Planas, E., "Analysis of the geometric and radiative characteristics of hydrocarbon pool fires," *Combust. Flame* 139:263-277, 2004.

Nakos, J. T., "Uncertainty analysis of thermocouple measurements used in normal and abnormal thermal environment experiments at Sandia's Radiant Heat facility and Lurance Canyon burn site," SAND2004-1023, April 2004, Sandia National Laboratories, Albuquerque, NM.

Nakos, J. T., "Uncertainty analysis of steady state incident heat flux measurements in hydrocarbon fuel fires," SAND2005-7144, December 2005, Sandia National Laboratories, Albuquerque, NM.

Novozhilov, V., and Koseki, H., "CFD prediction of pool fire burning rates and flame feedback," *Combust. Sci. and Tech.* 176:1283-1307, 2004.

Orloff, L., and de Ris, J., "Froude modeling of pool fires," Proceedings of the 19th Symposium (International) on Combustion, 1982, pp. 885 – 895.

Pouchert, C. J., *The Aldrich library of FT-IR spectra*, Volumes 1 through 3, Aldrich Chemical Company, Milwaukee, WI, 1985.

Prasad, K., Li, C., Kailasanath, K., Ndubizu, C., Ananth, R., and Tatem, P. A., "Numerical modeling of methanol liquid pool fires," *Combust. Theory Modelling* 3:743-768 (1999).

Ricks, A. J., "Characterization of air flow in New FLAME / Radiant Heat," Sandia internal memo to T. Blanchat, March 20, 2006.

Ricks, A. J., "Results of calibration tests of FM Global cold heat flux pipes," Informal communication from Tom Blanchat, Sandia National Laboratories to John de Ris, FM Global Research, 2006.

Ricks, A., Blanchat, T., and Jernigan, D., "Validation experiments to determine radiation partitioning of heat flux to an object in a fully turbulent fire," SAND2006-3494, June 2006, Sandia National Laboratories, Albuquerque, NM.

Romero, V. J., Sherman, M. P., Johnson, J. D., Dempsey, J. F., Edwards, L. R., Chen, K. C., Baron, R. V., and King, C. F., "Development and validation of a component failure model," paper AIAA2005-2141, *46th AIAA/ASME/AHS/ASC Structures, Structural Dynamics, and Materials Conference*, April 18-21, 2005, Austin, TX.

DISTRIBUTION

External

1 John L. de Ris
FM Global Research
1151 Boston-Providence Hwy.
Norwood, MA 02062

1 Benjamin Ditch
FM Global Research
1151 Boston-Providence Hwy.
Norwood, MA 02062

Internal

1	MS0384	A.C. Ratzel	1500
1	MS0821	A.L. Thornton	1530
1	MS1135	S.R. Tiezsen	1532
5	MS1135	T.K. Blanchat	1532
1	MS1135	A.J. Ricks	1532
1	MS0836	W. Gill	1532
1	MS1135	J.T. Nakos	1532
1	MS1135	J.M. Suo-Anttila	1532
1	MS1135	V.F. Nicolette	1532
1	MS1135	D.A. Jernigan	1532
1	MS1135	S. Gomez	1532
1	MS1135	A.L. Brown	1532
1	MS0836	C.A. Glissman	1532
1	MS0828	M. Pilch	1544
1	MS0828	V.J. Romero	1544
1	MS0828	A.R. Black	1544
1	MS0834	R.D. Tachau	1512
1	MS0834	T.J. O'Hern	1512
1	MS0834	S.P. Kearney	1512
1	MS0382	S.G. Gianoulakis	1541
1	MS0382	S.P. Domino	1541
1	MS9409	C. Moen	8757
2	MS9018	Central Technical Files	8944
2	MS0899	Technical Library	4536